Numerical analysis of beam parameters and stability regions in a folded or ring cavity

Xinglong Wang, Guojiang Hu, Yu Li, and Jianquan Yao

Department of Precision Instrument Engineering, Tianjin University, Tianjin 300072, China

Received October 5, 1992; revised manuscript received March 25, 1994; accepted March 28, 1994

A numerical method for analyzing a folded or ring cavity is presented. Astigmatic compensated parameters, stability regions, and beam parameters inside the cavity or within the gain medium can be obtained numerically as long as the intracavity beam propagation can be expressed by round-trip matrices, no matter how complicated the cavity is. This method is easy to follow, and the results are accurate.

Key words: transfer matrix, *ABCD* law, astigmatic compensation, stability region, beam parameter

INTRODUCTION

In dye or Ti^{3+}:Al_2O_3 laser applications there is a need for cavity designs that provide intracavity focuses where the beam is highly concentrated. These small spots are required for laser pumping, saturable absorber action, frequency-doubled crystal action, and cavity dumping by acousto-optic crystals. Cavities with configurations that satisfy the requirement of long length and tight focusing are resonators with internal lenses or, equivalently, cavities with folded arms. Kogelnik *et al.*[1] analyzed in detail the folded three-mirror cavity. Li *et al.*[2] and Li[3] computed folded five- and six-mirror cavities by using an overall matrix. Siegman described how to solve the problem of laser resonators, using an overall matrix.[4] Metcalf *et al.*, using this method, solved laser resonators containing self-focusing elements.[5]

The cavity considered here may be a three- or four-mirror cavity or any other complicated cavity consisting of one or several focusing arms, and some of these arms may contain planar jet streams or Ti^{3+}:Al_2O_3 crystals or other compensated plates. A clear understanding of the stability regions of the cavity, the thickness(es) of the compensated plate(s), and the beam parameters inside the cavity and within the compensated plate(s) is important for the design or alignment of this cavity.

NUMERICAL METHOD

Astigmatic Elements

A Brewster cell, or Brewster angle window, acts differently in the tangential and the sagittal planes. The transfer matrices of the tilted plate in the two planes are described by $\mathbf{T}_T$ and $\mathbf{T}_S$,[6] respectively:

$$\mathbf{T}_T = \begin{bmatrix} 1 & H\sqrt{n^2+1}/n^4 \\ 0 & 1 \end{bmatrix}, \tag{1}$$

$$\mathbf{T}_S = \begin{bmatrix} 1 & H\sqrt{n^2+1}/n^2 \\ 0 & 1 \end{bmatrix}, \tag{2}$$

where H is the thickness of the plate and n is the refractive index of the plate.

It is well known that a concave mirror used at oblique incidence focuses tangential ray bundles at a location different from that of sagittal bundles. This is reflected in two different effective focal lengths, f_T and f_S:

$$f_T = R\cos\theta/2, \tag{3}$$

$$f_S = R/2\cos\theta, \tag{4}$$

where θ is the angle of incidence and R is the curvature radius of the mirror.

Cavity Stability Condition and Astigmatism-Compensated Criterion

Numerical calculations were carried out with use of the complex Gaussian beam parameter q and the *ABCD* matrix of each of the cavity elements in sequence. Dye streams, titanium sapphire crystals, or any other compensated plate cannot be neglected in the calculation. Self-consistency is required for stability. The result is[7]

$$\frac{1}{q} = \frac{D-A}{2B} - j\frac{\left[1-\left(\frac{D+A}{2}\right)^2\right]^{1/2}}{B} = \frac{1}{r} - j\frac{\lambda}{\pi\omega^2}. \tag{5}$$

Hence the beam equiphase curvature radius r and spot size ω are

$$r = \frac{2B}{D-A}, \tag{6}$$

$$\omega = \left\{\frac{\lambda|B|}{\pi\left[1-\left(\frac{D+A}{2}\right)^2\right]^{1/2}}\right\}^{1/2}. \tag{7}$$

In the computer analysis the mirrors, empty spaces, and dye streams or any other compensated plates are presented by separate matrices. The starting and ending points are selected on one particular position (which may be the output mirror or any other place) of the cavity. In one round trip the overall matrix is

0740-3232/94/082265-06$06.00

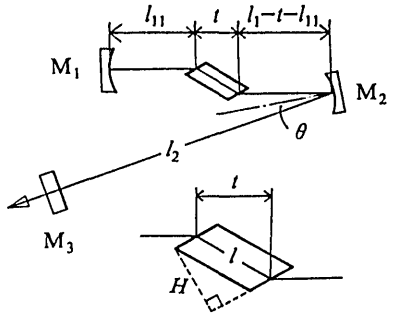

Fig. 1. Folded three-mirror cavity with compensated plate.

$$\mathbf{M}_0 = \begin{bmatrix} A_0 & B_0 \\ C_0 & D_0 \end{bmatrix}. \tag{8}$$

The usual stability condition is[7]

$$-1 < \frac{D_0 + A_0}{2} < 1. \tag{9}$$

For convenience we define parameter $G = (D_0 + A_0)/2$. It is clear that the cavity is extremely stable when G is in the vicinity of zero and that the cavity approaches instability when $G \simeq \pm 1$.

Because of astigmatic effects, the complex Gaussian beam parameter q, the *ABCD* matrix, the defined stability parameter G, and the beam parameters ω and r are different in the tangential and the sagittal planes. When the cavity astigmatism is compensated on the output mirror, there will be

$$\omega_T = \omega_S, \tag{10}$$

$$r_T = r_S, \tag{11}$$

where ω_T, ω_S and r_T, r_S are the beam spot radii and the equiphase curvature radii, respectively, in the two planes. We consider Eqs. (10) and (11) the criteria of one cavity by which the astigmatism from the output mirror is or is not compensated.

STABILITY REGIONS OF FOLDED THREE- AND FOUR-MIRROR CAVITIES

Folded Three-Mirror Cavity

The three-mirror cavity, illustrated in Fig. 1, is one of the simplest configurations for giving tight focus, as is required in a dye or a titanium sapphire laser.

The thickness of the compensated plate (the plate may be a dye stream, a titanium sapphire crystal, or any other planar plate) is H, its length along the light traveling direction is l, and the spacing length along the arm direction is t (as shown in Fig. 1). M's denote mirrors. Using principles of geometrical optics, we derive

$$t = \frac{2H}{(n^2 + 1)^{1/2}}, \tag{12}$$

$$l = \frac{(n^2 + 1)^{1/2}}{n} H. \tag{13}$$

When all factors, including the mirrors, empty spaces, and the compensated plate, in one round trip, are taken into account, the *ABCD* matrix (assuming mirror M_3 as the starting and ending point) is

$$\begin{aligned} \mathbf{M} = &\begin{bmatrix} 1 & 0 \\ 0 & 1 \end{bmatrix}\begin{bmatrix} 1 & l_2 \\ 0 & 1 \end{bmatrix}\begin{bmatrix} 1 & 0 \\ -\frac{1}{f_2} & 1 \end{bmatrix}\begin{bmatrix} 1 & l_1 - t - l_{11} \\ 0 & 1 \end{bmatrix} \\ &\times \mathbf{T}\begin{bmatrix} 1 & l_{11} \\ 0 & 1 \end{bmatrix}\begin{bmatrix} 1 & 0 \\ -\frac{2}{R_1} & 1 \end{bmatrix}\begin{bmatrix} 1 & l_{11} \\ 0 & 1 \end{bmatrix} \\ &\times \mathbf{T}\begin{bmatrix} 1 & l_1 - t - l_{11} \\ 0 & 1 \end{bmatrix}\begin{bmatrix} 1 & 0 \\ -\frac{1}{f_2} & 1 \end{bmatrix}\begin{bmatrix} 1 & l_2 \\ 0 & 1 \end{bmatrix}, \end{aligned} \tag{14}$$

where matrix $\mathbf{T}$ and focal length f_2 are replaced by Eqs. (1) and (3), respectively, in the tangential plane and by Eqs. (2) and (4), respectively, in the sagittal plane. l_{11} is the free-space distance from the Brewster plate to mirror M_1. R_1 and R_2 are curvature radii of the end mirror M_1 and the folding mirror M_2, respectively. We note that

$$\mathbf{M} = \mathbf{M}_1\mathbf{M}_2 \cdots \mathbf{M}_{12} = \begin{bmatrix} A_0 & B_0 \\ C_0 & D_0 \end{bmatrix},$$

$$\mathbf{M}' = \mathbf{M}_7\mathbf{M}_8\mathbf{M}_9 \cdots \mathbf{M}_{12} = \begin{bmatrix} A_1 & B_1 \\ C_1 & D_1 \end{bmatrix},$$

$$\mathbf{M} = \mathbf{M}_1\mathbf{M}_2 \cdots \mathbf{M}_6\mathbf{M}',$$

and obtain

$$\begin{aligned} A_1 &= 1 - \frac{k}{f_2}, \\ B_1 &= l_2 + k - \frac{l_2 k}{f_2}, \\ C_1 &= -\frac{1}{f_2} - \frac{2A_1}{R_1}, \\ D_1 &= 1 - \frac{l_2}{f_2} - \frac{2B_1}{R_1}, \end{aligned} \tag{15}$$

$$\begin{aligned} D_0 &= D_1 - \frac{B_1 + kD_1}{f_2}, \\ C_0 &= C_1 - \frac{A_1 + kC_1}{f_2}, \\ B_0 &= B_1 + kD_1 + l_2D_0, \\ A_0 &= A_1 + kC_1 + l_2C_0, \end{aligned} \tag{16}$$

where

$$k = \begin{cases} l_1 - t + H\sqrt{n^2 + 1}/n^4 & \text{for the tangential plane} \\ l_1 - t + H\sqrt{n^2 + 1}/n^2 & \text{for the sagittal plane} \end{cases}. \tag{17}$$

Inspecting Eqs. (15)–(17), we find that l_{11} does not exist in these equations; i.e., the cavity stability and the beam parameters at the output mirror are not affected by the

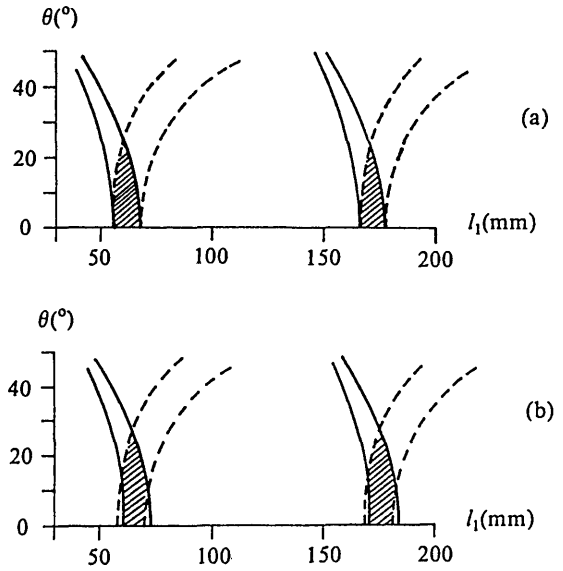

Fig. 2. Stability regions of a folded three-mirror cavity. Solid and dashed curves represent regions in the tangential and the sagittal planes, respectively. Intersections are the stability regions. Parameters are $l_2 = 300$ mm, $R_1 = R_2 = 110.4$ mm, $n = 1.77$, and $\lambda = 0.79$ μm; the thickness of the compensated plate is (a) $H = 0$, (b) $H = 8$ mm ($l = 9.19$ mm).

position of the compensated plate (between mirrors M_1 and M_2).

Computations are made separately in the two planes, and the overlapped region is identified as the stable region. A typical result is shown in Fig. 2. Solid and dashed curves indicate the tangential and the sagittal planes, respectively. The sensitive parameters are the length of the folded arm l_1 and the folding angle θ, which form a system of rectangular coordinates. As we can see from Fig. 2, the widest adjustable measurement of the sensitive arm length l_1 corresponds to a specific folding angle, and this result is the same as the analytic solution.[1]

There are two stability regions in each of the figures. The right-hand stability region is usually used in dye laser applications, and we find that the left-hand region may be used also. The two stability regions in Fig. 2(b) are compared as follows:

Right-hand region: Typical cavity parameters are $\theta = 13°$, $l_1 = 177$ mm, $l_2 = 300$ mm, and $R_1 = R_2 = 110.4$ mm; the output beam parameters are $\omega_T = 0.2277$ mm, $\omega_S = 0.2281$ mm, $r_T = r_S = \infty$, $G_T = -0.0713$, and $G_S = -0.0432$.

Left-hand region: Typical cavity parameters are $\theta = 13.2°$, $l_1 = 64.9$ mm, $l_2 = 300$ mm, and $R_1 = R_2 = 110.4$ mm; the output beam parameters are $\omega_T = 0.2765$ mm, $\omega_S = 0.2768$ mm, $r_T = r_S = \infty$, $G_T = -0.1049$, and $G_S = -0.1058$.

Clearly each of the two stability regions can be used. We note that the astigmatism will still exist in the output beam when the thickness of the compensated plate and the folding angle satisfy the analytic solution[1] if the sensitive parameter l_1 is not suitable. Furthermore, we find that the position of the left-hand region is fixed and that the position of the right-hand region shifts to the right when the curvature radius of mirror M_2 is fixed and the curvature radius of mirror M_1 increases. If $R_1 = \infty$ the right-hand region will disappear, and the waist of the left-hand region will be on mirror M_1. An end-pumped laser resonator as used by Maker[8] is an example of the configuration. This kind of resonator has been widely used for diode laser end-pumped solid-state lasers.

Folded Four-Mirror Cavity

Most of astigmatic cavities used for the purposes of continuous-wave operation are longitudinally pumped by high-power blue-green lasers. The resonator is difficult to align because the near-infrared fluorescence of the active media is concealed by pumping light onto each mirror of a folded three-mirror cavity, and the stability region of this cavity is small. In contrast, there is no pumping light on the output mirror, and the stability region of a folded four-mirror cavity is large. So a folded four-mirror cavity, shown in Fig. 3, has been used for passively mode-locked or self-mode-locked dye or titanium sapphire lasers. Parameters l_1, l_2, and l_3 are lengths of the three arms, and R_2 and R_3 are curvature radii of mirrors M_2 and M_3. For convenience, the starting and ending points are on output mirror M_1.

Figure 4 shows the computer solutions for the stability regions of the four-mirror cavity with the astigmatism compensated. As shown in Fig. 4(a), the stability region is an entire region when l_1 is equal to l_3; but the entire stability region is immediately divided into four portions, as there is very little deviation between arm lengths l_1 and l_3, as shown in Fig. 4(b). Therefore some areas in the stability region shown in Fig. 4(a) are not very stable, even though the stability region is a large and whole region. One must pay more attention to this fact when one is designing or aligning a folded four-mirror cavity.

The result can easily be generalized to other cases. The stability regions and thicknesses of the compensated plates of any complicated cavity with several concave mirrors and compensated plates can be calculated precisely as long as the beam propagation inside the cavity can be expressed by round-trip matrices.

BEAM PARAMETERS INSIDE THE CAVITIES

If the starting and ending points are selected at various places inside the cavity, the overall matrices at various places inside the cavity can be worked out, and the beam parameters inside the cavity can be calculated. Figure 5 shows spot size versus position for the folded three-mirror cavity shown in Fig. 1. As can be seen from Figs. 5(b) and 5(c), astigmatism is eliminated in the output beam

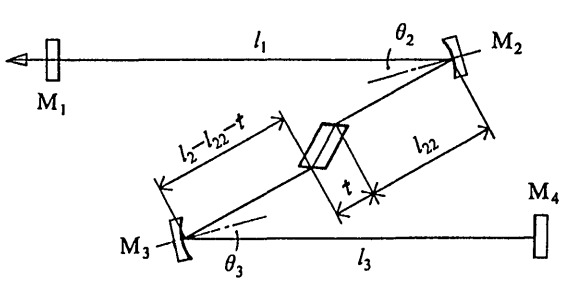

Fig. 3. Folded four-mirror cavity with a compensated plate.

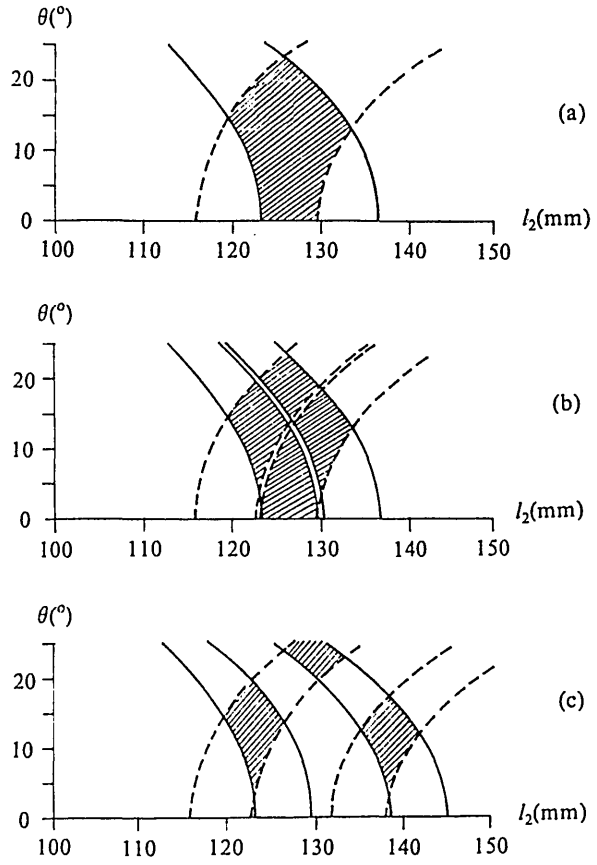

Fig. 4. Stability regions of a folded four-mirror cavity. The cavity parameters are $R_1 = R_4 = \infty$, $R_2 = R_3 = 110.4$ mm, $H = 16.54$ mm ($l = 19$ mm), $n = 1.77$, $\lambda = 0.79$ μm. (a) $l_1 = l_3 = 500$ mm, (b) $l_1 = 500$ mm, $l_3 = 480$ mm, (c) $l_1 = 500$ mm, $l_3 = 250$ mm.

but not within the gain medium itself; i.e., the beam waist in the sagittal plane is not equal to the beam waist in the tangential plane.

Calculations of the beam parameters within the compensated plate (i.e., gain medium, frequency doubled crystal, or any other compensated plate) are complicated. Figure 6 indicates a beam propagated from free space to the compensated plate. Using the principles of geometry, we obtain

$$\omega_T' = n\omega_T, \tag{18}$$

$$\omega_S' = \omega_S, \tag{19}$$

where ω_T, ω_S are radii of the incident beam and ω_T', ω_S' are radii of the refracted beam at the boundary plane.

Figure 7 shows the beam spot distribution within the compensated plate. P_1, P_2, P_1', and P_2' are the reference planes at the surfaces of the compensated plate. P_1 and P_1', P_2 and P_2' are close together, as shown.

We know that the envelope curve of a fundamental Gaussian-beam radius within the compensated plate in the tangential or sagittal plane is a hyperbola curve, and its equation is

$$\frac{\omega^2}{\omega_0^2} - \frac{z^2}{f^2} = 1, \tag{20}$$

where

$$f = \frac{\pi\omega_0^2}{\lambda}, \tag{21}$$

z is the transverse coordinate along the resonator axis

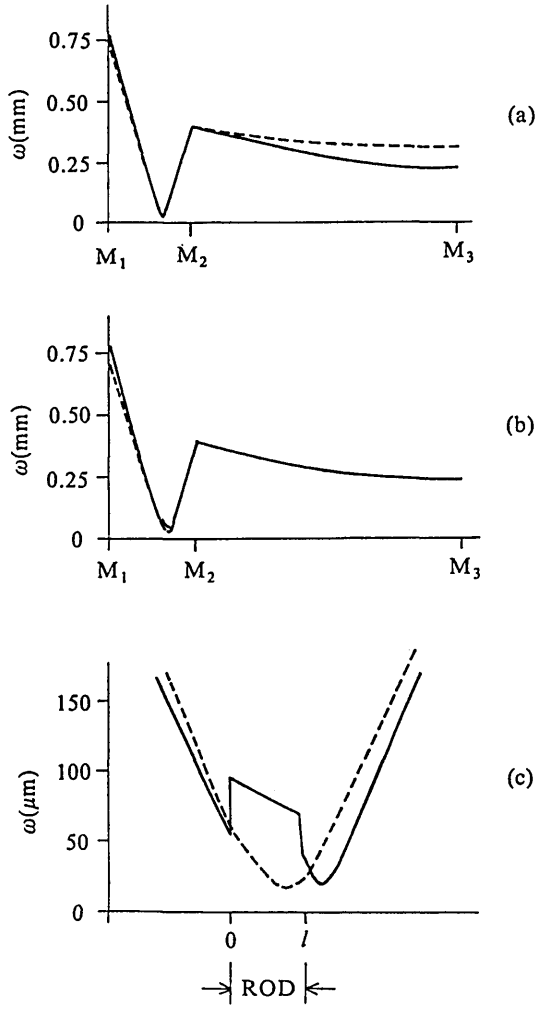

Fig. 5. Folded three-mirror-cavity beam spot size versus position in the tangential and sagittal planes. The beam spot size is defined at the e^{-2} points of the Gaussian intensity profile. Solid and dashed curves represent sizes in the tangential and sagittal planes, respectively. Parameters are $l_2 = 300$ mm, $R_1 = R_2 = 60.395$ mm. (a) $l_1 = 92.2$ mm, $\theta = 10°$, and $H = 0$ (i.e., the cavity is empty); (b) $l_1 = 97$ mm, $\theta = 18.3°$, and the compensated-plate thickness $H = 8$ mm ($l = 9.19$ mm); (c) expanded view of the cavity spot sizes at the compensated plate. Parameters are the same as in (b). The discontinuity in the spot size in the tangential plane at the ends of the rod is caused by the beam's entry into the rod at the Brewster angle and the resultant beam deviation at the rod surfaces. A slight discontinuity in the slope of the spot size in the sagittal plane is due to the discontinuity of the beam curvature radius from free space to the titanium sapphire crystal.

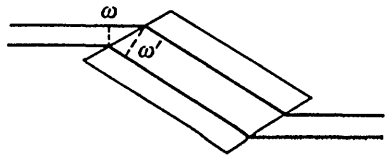

Fig. 6. Beam propagated from free space to the Brewster-angle compensated plate. ω and ω' are radii of the incident beam and the refracted beam, respectively.

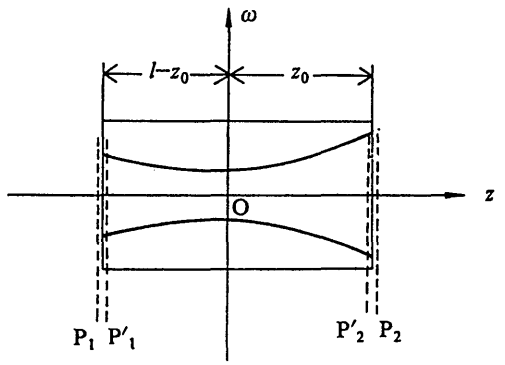

Fig. 7. Distribution of the Gaussian-beam spot size within the compensated plate. P_1, P_1', P_2, and P_2' are reference planes at the boundary planes; they are parallel to each other. $(l - z_0)$ and z_0 are distances from P_1 and P_2, respectively, to the beam waist.

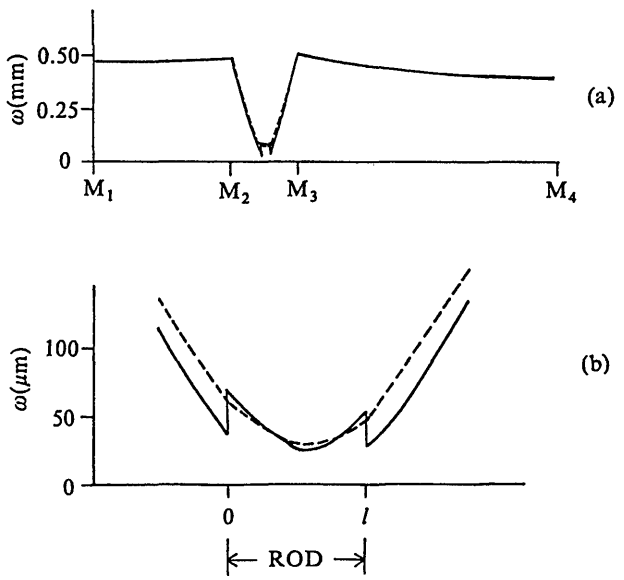

Fig. 8. Folded four-mirror-cavity beam spot size versus position in the tangential and sagittal planes. Parameters are $l_1 = 250$ mm, $l_2 = 122.6$ mm, $l_3 = 500$ mm, and $\theta = 14.3°$; other parameters are the same as in Fig. 4. (a) Beam spot sizes inside the cavity; (b) expanded view of the cavity beam spot sizes at the compensated plate.

($z = 0$ at the beam waist), ω_0 is the beam-waist radius, and λ is the light wavelength in the compensated plate.

The beam parameters in the reference planes P_1 and P_2 can be obtained if the starting and ending points of the overall matrices are selected separately in these two reference planes. Combining Eqs. (18)–(21), we can obtain the parameters ω_0, z_0, and f. So the beam-radius envelope within the compensated plate can be obtained, as shown in Fig. 5(c).

The beam parameters ω_T', ω_S', r_T', and r_S' in the reference planes P_1' and P_2' can be obtained also in terms of the radius ω_0 and the location z_0 of the beam waist given above by use of the propagation theory of the Gaussian beam[7]:

$$\omega(z) = \omega_0\left[1 + \left(\frac{\lambda z}{\pi\omega_0^2}\right)^2\right]^{1/2}, \tag{22}$$

$$r(z) = z\left[1 + \left(\frac{\pi\omega_0^2}{\lambda z}\right)^2\right], \tag{23}$$

and then we have the following relationships:

$$\frac{r_T'}{r_T} = C_T, \tag{24}$$

$$\frac{r_S'}{r_S} = C_S, \tag{25}$$

where C_T and C_S are related to many parameters (position of the beam waist, radius of the beam waist, wavelength of the light, refractive index of the compensated plate, etc.), and their results can be calculated easily according to Eqs. (24) and (25). Usually C_T and C_S are not equal to 1; i.e., the beam equiphase curvatures are discontinuous in tangential and sagittal planes. We consider Eqs. (18), (19), (24), and (25) the boundary relationships of the fundamental Gaussian beams between two different mediums.

Alfrey[9] discussed the beam parameters within the gain medium, but he did not present a clear method, and with his method he calculated the beam parameters in the gain medium.

Figure 8 shows the spot-size distribution at various places inside the folded four-mirror cavity that is shown in Fig. 3.

CONCLUSION

A complicated cavity, for example, a four-mirror ring cavity with three concave mirrors, cannot be solved exactly by an analytic solution. We proposed a useful numerical method on the basis of the theory of fundamental Gaussian beams. Folded three- and four-mirror cavities are analyzed here both analytically and numerically. The results are quite useful in the design and alignment of the laser cavities.

The thickness(es) of the compensated plate(s), folding angle(s), stability regions, and beam parameters inside the cavities and within the compensated plate(s), as well as any other sensitive parameters, all of which are results of the cavity parameters and their variation ranges (generalized as stability regions), can be obtained numerically with this method.

Any complicated astigmatic cavity with one or several folding mirrors and compensated plates can be analyzed numerically with this method as long as the beam propagation inside the cavity can be expressed by round-trip matrices. This numerical method is simple and the results are precise.

The key to this method is that the transfer matrix of the compensated plate is taken into consideration in the overall matrix.

ACKNOWLEDGMENT

The authors express their appreciation to the reviewers for suggesting a number of significant improvements.

REFERENCES

1. H. W. Kogelnik, E. P. Ippen, A. Diencs, and C. V. Shank, "Astigmatically compensated cavities for CW dye lasers," IEEE J. Quantum Electron. **QE-8**, 373–379 (1972).
2. K. Li, A. Dienes, and J. R. Whinnery, "Stability and astigmatic compensation analysis of five-mirror cavity for mode-locked dye lasers," Appl. Opt. **20**, 407–411 (1981).

3. K. Li, "Stability and astigmatic analysis of a six-mirror ring cavity for mode-locked dye lasers," Appl. Opt. **21,** 967–970 (1982).
4. A. E. Siegman, *Lasers* (University Science Books, Mill Valley, Calif., 1986), Chap. 15, p. 581; Chap. 21, p. 815.
5. D. Metcalf, P. de Giovanni, J. Zachorowski, and M. Leduc, "Laser resonators containing self-focusing elements," Appl. Opt. **26,** 4508–4517 (1987).
6. D. C. Hanna, "Astigmatic Gaussian beams produced by axially asymmetric laser cavities," IEEE J. Quantum Electron. **QE-5,** 483–488 (1969).
7. H. Kogelnik and T. Li, "Laser beams and resonators," Appl. Opt. **5,** 1550–1567 (1966).
8. G. T. Maker, S. J. Keen, and A. I. Fergnson, "Mode-locked and Q-switched operation of a diode laser pumped Nd:YAG laser operating at 1.064 μm," Appl. Phys. Lett. **53,** 1675–1677 (1988).
9. A. J. Alfrey, "Modeling of longitudinally pumped CW Ti:sapphire laser oscillators," IEEE J. Quantum Electron. **25,** 760–766 (1989).